Supplementary Material

Supplementary Method

Region-based source analysis

EEG source analysis was done following the procedures introduced by (Jonmohamadi et al. 2014) and detailed in our previous paper (Gong et al. 2021). In brief, the raw data from EEG sensor signals were projected on the cortical surface employing individual head models and a linearly constrained minimum variance beamformer method (Van Veen and Buckley 1988) to obtain the source signal in each specific brain region. A combination of principal component analysis (PCA) and independent component analysis (ICA) was applied to obtain signals from components with relatively independent spatiotemporal characteristics in a specific region. In specific, PCA was first applied to determine the number of components and reduce the noise by keeping the main components which can explain 95% of the data variance. And then ICA was used to obtain spatiotemporally independent components in each region. Each component could represent a sub-network in that region. We calculated a common beamformer filter under the merged data of all conditions and applied the PCA-ICA procedure separately to each of the 6 conditions. The PCA-ICA weights were then applied back on the artifacts-marked source signals of the 6 conditions. This study investigated the 4 brain regions that we previously found to show statistically enhanced PAC in PD patients compared with controls (Gong et al. 2021). These regions were the premotor cortex (PMC), the primary motor cortex (M1), the primary somatosensory cortex (BA3), and the primary somatosensory complex (BA1&2), which were defined with reference to the multi-model parcellation of Glasser et al. (Glasser et al. 2016). The information regarding the average number of components of each region in patients and controls the 6 conditions are provided in Table S3.

Definition of 4 trigger points of a movement cycle

The definition of 4 peripheral movement trigger points. In order to investigate the dynamics of brain activities during transitions between movement states, we first determined in each subject when movement transitions occurred between different

movement phases. Therefore, we separated the movement into five periods divided by four trigger points. The four trigger points were first approximately derived from the digital kinetic (pressing) or kinematic (tapping) signals recorded during the movement for each individual for practical purpose (the peripheral movement trigger points). Trigger points were established individually for each movement cycle in each task. Since the movement transient is too quick during the fast tapping task to be segmented, this part of the analysis included exclusively the pressing and slow tapping tasks.

For the pressing task, the four peripheral movement trigger points were defined by the fixed force threshold and the maximum force the device could detect, as: 1) the movement onset – the time when the force level exceeding 1.3N; 2) the end of the force build-up – the moment when the pressing force exceeded the maximally detectable force of the device (4.4N); 3) the start of releasing – the detected start of releasing that was defined as the moment when the force fell below 4.4 N; 4) and the movement offset – the time when the force level falling below 1.3N. In some cases when the pressing force of a subject did not exceed the maximally detectable force of the device (4.4N), the end of the force build-up and the start of releasing were defined by the slope of the force signal, respectively, i.e., the end of force build-up was defined as the time when the signs of the force slope changed from at least two consecutive positive signs to 0 or negative (which means that the movement was changed from a continuous increasing state to the constant pressing or releasing state), while the start of releasing was defined as the moment the sign of the slope changed from 0 or positive to at least two consecutive negative signs (which means that the movement was changed from a constant pressing state to a releasing state).

For the tapping task, the four peripheral movement trigger points were defined based on the lower and upper photoelectric sensors as 1) movement onset – the time when the index finger had reached the height of the lower photoelectric sensor; 2) the end of finger extension – the time when the index finger had been extended up to the height of the upper photoelectric sensor; 3) the start of finger flexion – the time when the index finger had been lowered below the upper photoelectric sensor; 4) the movement offset – the time when the index finger had been lowered below the lower photoelectric sensor.

Measurement of the general delay. Importantly, to estimate the timing of the transition times at the cortex level at the best possible accuracy, we defined the cortical movement trigger points based on the peripheral movement trigger points by further taking into account the influence of the general delay, including the general mechanical, electromechanical delays and the corticomuscular conduction time, across subjects in pressing and tapping events. The electromechanical delay is the time delay between the onset of muscle activation and the measurable movement, reflecting both electrochemical and mechanical processes, previously demonstrated to be around 50ms (Cavanagh and Komi 1979). And the corticomuscular conduction time was defined as the time lag from the activation of the motor cortex to the activation of muscle, which was measured as 20ms in general, as demonstrated by the TMS experiment (Samii et al. 1998).

For practical purposes, peripheral movement onset and offset were defined by the time of passing the lower force threshold for pressing tasks or the activation of the lower light beam sensor for tapping tasks, as described above. However, using fixed force values and light sensors as start and end markers has a common disadvantage; the subjects are likely to have started the movement before or stopped it afterward. Therefore, to minimize the bias, the mechanical delay was defined as the delay from the computed movement onset/offset to the peripheral movement events as practically determined by the fixed force threshold or photoelectric sensor signal. We used kinetic signals recorded from the force transducer in both pressing tasks and slow tapping tasks to assess the computed movement onset and offset objectively.

In terms of processing the kinetic signals recorded from the force transducer, for each subject, the signals were first segmented into 3s epochs (-1s before the peripheral movement onset/offset and 2s after the peripheral movement onset/offset). Then the signals were interpolated to bring the sampling rate to the same value (2kHz). An averaged digital signal across epochs was calculated for each subject. Because the frequency of the movements for pressing and slow tapping tasks was considerably lower than 5Hz for our cohort, the signals were smoothed through a low pass Butterworth filter at 10Hz (2nd order) to avoid interference from high-frequency activities.

Measurement of the general mechanical delay in pressing task. We determined the computed movement onset for pressing movements when pressure acceleration reached the maximum and the computed movement offset as the time when pressure acceleration reached the minimum. To this end, we calculated the second derivative of the digital signals in every 10ms window with a 5ms time step. The computed movement onset/offset was then determined at the location of the peak (local maximum) close to 0ms (the peripheral movement onset), or the location of the valley (local minimum) close to 0ms (the peripheral movement offset), as shown in Fig. S2A&B (left panel), respectively. The mechanical delay for each subject on the movement onset/offset is given by the time differences between the computed onset/offset to the 0ms (the peripheral movement onset/offset). The general mechanical delay was then calculated as the averaged mechanical delay across subjects. In this way, the general mechanical delay at the movement onset was 43ms (Fig. S2A, right panel), while the general mechanical delay at movement offset was 9.8ms (Fig. S2B, right panel).

Measurement of the general mechanical delay in slow tapping task. For slow tapping movements, we determined the computed movement onset when the pressure rate reached the minimum, which indicated that the finger had left the pressure plate (One subject was excluded from the analysis because of the loss of the online records of the force transducer). Therefore, we calculated the first derivative of the digital signals in every 10ms window with a 5ms time step. The computed movement onset was then determined on the valley (local minimum) close to 0ms (the peripheral movement onset), as shown in Fig. S2C (left panel). Therefore, the general mechanical delay across subjects at the movement onset was calculated to be 60ms (Fig. S2C, right panel). As for the movement offset, we checked when the finger started to touch the pressure plate. We found a quick (<10ms) deflection of the force signal right after the finger flexion had crossed the lower light beam sensor (Fig. S2D). We neglected this delay at the movement offset because of its brevity.

The definition of cortical movement trigger points. Overall, in the pressing task, the general delay in total from the cortical movement onset to the peripheral movement onset of pressing was estimated as 113ms (20ms + 50ms + 43ms). The delay from the cortical movement offset to the peripheral movement offset of pressing was estimated as 60ms (20ms + 50ms -10ms). Besides, due to the force saturation (the maximum force that can be

detected is 4.5N) during the pressing in most cases, the realistic ending of pressing and start of releasing cannot be acquired, the delays for the two trigger points between the movement onset and offset only included the general electromechanical delay and the corticomuscular conduction time, which are 70ms. Therefore, for the pressing task, also considering the 50ms time resolution of the movement-PAC values, the 4 cortical movement trigger points were shifted from the peripheral movement triggers, respectively.

In the slow tapping task, the delay in total from the cortical movement onset to the peripheral movement onset of tapping was estimated as 130ms (20ms + 50ms + 60ms). The delay from the cortical movement offset to the peripheral movement offset of tapping only contains the general electromechanical delay and the corticomuscular conduction time, which in total was 70ms. Besides, because the device did not record the whole trace of the finger tapping when the finger left the pressing board, the delays for the two trigger points between the movement onset and offset only included the general electromechanical delay and the corticomuscular conduction time, which are 70ms. Therefore, for the slow tapping task, also considering the time resolution (50ms) of movement-related PAC time series, the 4 cortical movement trigger points were shifted from the peripheral movement triggers, respectively.

Supplementary Figure

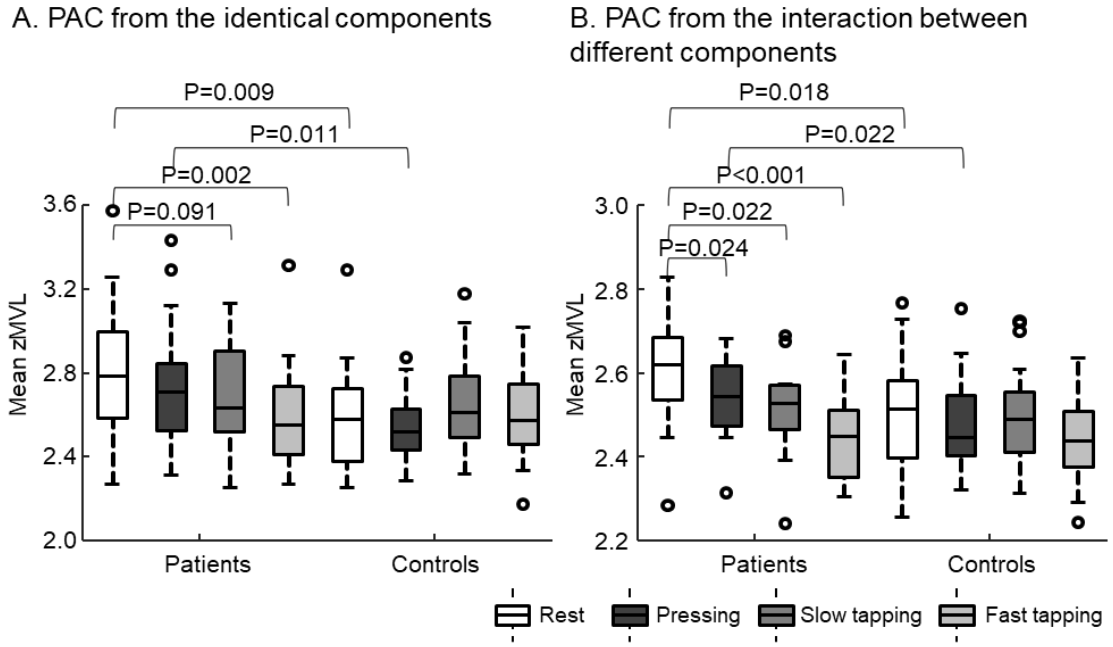

Fig. S1. State-related PAC computed from identical components and from the interaction between different components. Left, State-related PAC computed from identical components. A three-way nonparametric ANOVA showed significant interaction effects between Group and Tasks ($F(3,111)=5.4$, $P=0.002$). Post-hoc tests of the Group*Task interaction effect showed significant differences between the resting state and fast tapping task in the patients. Note that state-related PAC differed between patients and controls in resting state and during pressing. Right, State-related PAC computed from identical components. A three-way nonparametric ANOVA showed significant interaction effects between Group and Tasks ($F(3,111)=4.1$, $P=0.008$). Post-hoc tests of the Group*Task interaction effect showed significant differences between the resting state and all three movement tasks in the patients. Note that state-related PAC differed between patients and controls in resting state and during pressing. The results were similar to that of state-related PAC computed from the average across the whole pairwise matrix (n*n components).

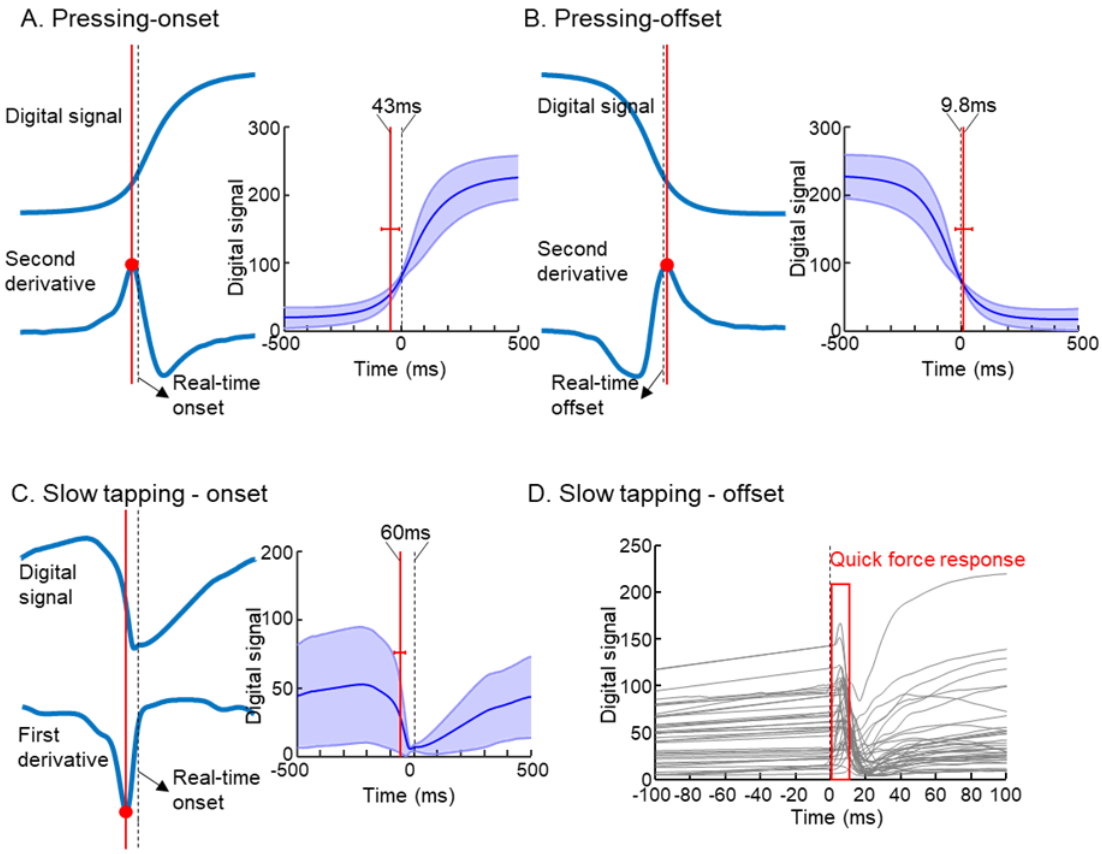

Fig. S2. Estimation of mechanical delay in pressing and slow tapping tasks via digital signals from force transducer. A. Mechanical delay at the movement onset of pressing task. Left, the computed movement onset was determined at the local maximum of the second derivative of the digital signals from the force transducer for each subject. Right, the general mechanical delay was estimated by the time difference between the peripheral movement onset (0ms point) and the averaged moments for computed movement onset across subjects. B. Mechanical delay at the movement offset of pressing task. Left, the computed movement onset was determined at the local maximum of the second derivative of the digital signals from the force transducer for each subject. Right, the general mechanical delay was estimated by the time difference between the peripheral movement offset (0ms point) and the averaged movements for computed movement offset across subjects. C. Mechanical delay at the movement onset of slow tapping task. Left, the computed movement onset was determined at the local minimum of the first derivative of the digital signals from the force transducer for each subject. Right, the general mechanical delay was estimated by the time difference between the peripheral movement onset (0ms point) and the averaged moments for computed movement onset across subjects. D. Mechanical delay at the movement offset of the slow tapping task. The line plot showed interpolated digital signals of all subjects. Most of the subjects showed a quick and large force response right after the finger flexion interrupted the lower light sensor (peripheral movement offset, 0ms point). The period from the peripheral movement offset to the deflection of the force transducer was neglected because of its brevity.

Supplementary Table

Table S1. Characteristics of patients with Parkinson's disease

ID	Sex	Disease Duration, years	Clinically more affected body side/ MDS-UPDRS III hemi-body-scores	Total MDS-UPDRS III (medication off)	L-Dopa equivalent dose mg/day
01	Male	4	Right/7	15	310
02	Female	1	Left/5	6	210
03	Male	1	Left/10	22	400
04	Female	3	Left/6	10	152
05	Male	1	Left/8	12	500
06	Male	4	Right/10	30	735
07	Male	12	Right/12	20	682.5
08	Female	11	Left/11	24	400
09	Male	3	Left/10	30	525
10	Male	2	Right/5	12	100
11	Female	4	Left/13	32	300
12	Female	6	Left/7	19	955
13	Male	12	Left/11	35	1395
14	Male	2	Right/6	11	355
15	Female	3	Left/15	26	930
16	Male	6	Right/10	20	400
17	Male	17	Right/12	29	1185
18	Male	2	Right/13	21	520
19	Male	6	Right/8	14	930

the table is adapted from Gong et al., Brain 2021, with permission (Gong et al. 2021)

Table S2. Number of epochs in each condition

	Resting	Pressing	Slow tapping, FB-	Slow tapping, FB+	Fast tapping, FB-	Fast tapping, FB+	p-value
Patients	105.6±12.1	104.9±26.3	110.2±26.3	110.8±25.5	101.4±15.2	99.4±14.8	>0.2
Controls	108.5±5.3	103.6±28.6	101.1±30.6	103.2±31.4	103.3±15.7	100.6±18.2	>0.06
p-value	0.36	0.99	0.21	0.39	0.34	0.35	

FB-: without feedback; FB+: with feedback

Table S3. Number of ICA components derived from ROI source signals

		Resting	Pressing	Slow tapping, FB-	Slow tapping, FB+	Fast tapping, FB-	Fast tapping, FB+
PMC	**Patients**	10.5±0.6	10.2±0.7	10.2±0.9	10.2±0.9	10.0±0.9	10.1±0.9
	Controls	10.7±0.7	10.5±0.5	10.8±0.8	10.6±0.7	10.4±0.8	10.3±0.9
M1	**Patients**	10.5±0.5	10.5±0.5	10.4±0.8	10.5±0.8	10.4±0.8	10.5±0.9
	Controls	10.7±0.7	10.6±0.8	10.5±0.8	10.5±0.8	10.3±0.9	10.3±0.9
BA3	**Patients**	10.6±0.7	10.7±0.7	10.6±1.0	10.5±0.9	10.4±1.0	10.5±0.9
	Controls	10.9±0.6	10.8±0.6	10.8±0.7	10.7±0.8	10.7±0.7	10.6±0.7
BA1&2	**Patients**	10.8±0.7	10.6±0.8	10.7±0.9	10.7±0.9	10.6±0.9	10.7±0.7
	Controls	11.0±0.7	10.9±0.7	10.9±0.8	10.9±0.7	10.7±0.8	10.8±0.8

PMC: Premotor cortex; M1: Primary motor cortex; BA3: Primary somatosensory cortex; BA1&2: Primary somatosensory complex; FB-: without feedback; FB+: with feedback

Supplementary References

Cavanagh PR, and Komi PV. Electromechanical delay in human skeletal muscle under concentric and eccentric contractions. *European journal of applied physiology and occupational physiology* 42: 159-163, 1979.
Glasser MF, Coalson TS, Robinson EC, Hacker CD, Harwell J, Yacoub E, Ugurbil K, Andersson J, Beckmann CF, and Jenkinson M. A multi-modal parcellation of human cerebral cortex. *Nature* 536: 171-178, 2016.
Gong R, Wegscheider M, Mühlberg C, Gast R, Fricke C, Rumpf J-J, Nikulin VV, Knösche TR, and Classen J. Spatiotemporal features of β-γ phase-amplitude coupling in Parkinson's disease derived from scalp EEG. *Brain* 144: 487-503, 2021.
Jonmohamadi Y, Poudel G, Innes C, and Jones R. Source-space ICA for EEG source separation, localization, and time-course reconstruction. *NeuroImage* 101: 720-737, 2014.
Samii A, Luciano CA, Dambrosia JM, and Hallett M. Central motor conduction time: reproducibility and discomfort of different methods. *Muscle & Nerve: Official Journal of the American Association of Electrodiagnostic Medicine* 21: 1445-1450, 1998.
Van Veen BD, and Buckley KM. Beamforming: A versatile approach to spatial filtering. *IEEE assp magazine* 5: 4-24, 1988.